ACS Catalysis
Letter
pubs.acs.org/acscatalysis

Nonaqueous Electrocatalytic Oxidation of the Alkylaromatic Ethylbenzene by a Surface Bound Ru^{V}(O) Catalyst

Aaron K. Vannucci, Zuofeng Chen, Javier J. Concepcion, and Thomas J. Meyer*

Department of Chemistry, University of North Carolina at Chapel Hill, Chapel Hill, North Carolina 27599, United States

Supporting Information

ABSTRACT: The catalyst $[Ru(Mebimpy)(4,4'-((HO)_2OPCH_2)_2bpy(OH_2)]^{2+}$, where Mebimpy is 2,6-bis(1-methylbenzimidazol-2-yl)pyridine and $4,4'-((HO)_2OPCH_2)_2bpy$ is 4,4′-bis-methlylenephosphonato-2,2′-bipyridine, attached to nanocrystalline Sn(IV)-doped In_2O_3 (nanoITO) electrodes (nanoITO|$Ru^{II}-OH_2^{2+}$) has been utilized for the electrocatalytic oxidation of the alkylaromatics ethylbenzene, toluene, and cumene in propylene carbonate/water mixtures. Oxidative activation of the surface site to nanoITO|$Ru^{V}(O)^{3+}$ is followed by hydrocarbon oxidation at the surface with a rate constant of $2.5 \pm 0.2\ M^{-1}\ s^{-1}$ ($I = 0.1$ M $LiClO_4$, $T = 23 \pm 2$ °C) for the oxidation of ethylbenzene. Electrocatalytic oxidation of ethylbenzene to acetophenone occurs with a faradic efficiency of 95%. H/D kinetic isotope effects determined for oxidation of ethylbenzene point to a mechanism involving oxygen atom insertion into a C−H bond of ethylbenzene followed by further $2e^-/2H^+$ oxidation to acetophenone.

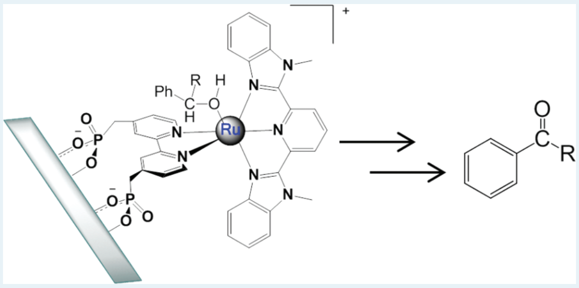

KEYWORDS: *polypyridyl ruthenium complexes, electrocatalysis, metal−oxo, hydrocarbon oxidation, nanoITO, surface catalysis*

1. INTRODUCTION

Alkylaromatic activation/oxidation has been investigated for a wide range of homogeneous catalysts, including transition metal porphyrins,[1,2] metal−oxo,[3−7] and metal−amine complexes[8] as well as Au nanocrystals.[9] Significant progress has also been made on a family of single-site ruthenium−oxo water oxidation catalysts in both homogeneous solutions and on modified electrode surfaces.[10−14] The latter undergo stepwise proton-coupled electron transfer (PCET) oxidative activation:

$$Ru^{II}{-}OH_2{}^{2+} \xrightarrow{-e^-/-H^+} Ru^{III}{-}OH^{2+} \xrightarrow{-e^-/-H^+} Ru^{IV}{=}O^{2+}$$

followed by $1e^-$ oxidation to $Ru^{V}{=}O^{3+}$.[13−15] The known water oxidation catalyst $[Ru(Mebimpy)(bpy)(OH_2)]^{2+}$ (**1**) (Mebimpy is 2,6-bis(1-methylbenzimidazol-2-yl)pyridine and bpy is 2,2′-bipyridine) has also been shown to electrocatalytically oxidize alcohols in homogeneous solution and as a heterogeneous system.[16,17] Here, we report the catalytic oxidation of the alkylaromatics ethylbenzene, toluene, and cumene on nanocrystalline Sn(IV)-doped In_2O_3 (nanoITO) electrodes derivatized with the phosphonated catalyst $[Ru(Mebimpy)(4,4'-((HO)_2OPCH_2)_2bpy(OH_2)]^{2+}$ (**1-PO$_3$H$_2$**) where $4,4'-((HO)_2OPCH_2)_2bpy$ is 4,4′-bis-methlylenephosphonato-2,2′-bipyridine, Scheme 1. The heterogeneous catalysts reported here exhibit excellent faradic efficiencies along with kinetics that are 2 orders of magnitude greater than related Ru(O) catalysts.[7,18]

Scheme 1. Oxidation Activation of nanoITO|1-PO$_3$H$_2$

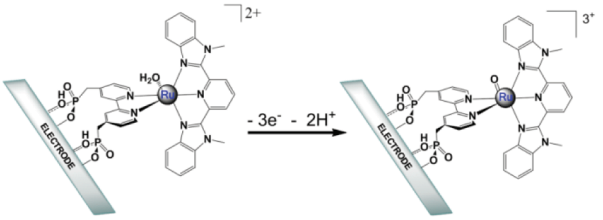

The synthesis and characterization of **1-PO$_3$H$_2$** has been reported elsewhere.[19] High-surface-area nanoITO electrodes were prepared according to literature procedures and had an average thickness of 2.5 μm with a resistance of ~200 Ω across a 1 cm section of the film.[20] Surface loading of **1-PO$_3$H$_2$** onto nanoITO occurred by soaking the slides overnight in methanol solutions containing 0.1 mM **1-PO$_3$H$_2$**. Absorption isotherms for this system have been previously reported.[12] Propylene carbonate (PC) was the solvent of choice for this study because of its oxidative stability up to 2.0 V vs NHE, miscibility with hydrocarbon substrates, weak coordinating properties, and partial miscibility with water (up to 8% by volume), which is required to sustain oxo-based catalytic cycles.[12] Although hydrolysis of propylene carbonate under acidic conditions is

Special Issue: Electrocatalysis

Received: January 18, 2012
Revised: March 15, 2012
Published: March 19, 2012

known, the reaction typically requires elevated temperatures and occurs more rapidly in base.[21] Cyclic voltammograms (CVs) were recorded in PC solutions containing 1% by volume H_2O and 0.1 M $LiClO_4$ as supporting electrolyte under atmospheric conditions without any degassing unless noted. Solutions were prepared for GC spectra collection by drying the solutions with $MgSO_4$. All current-vs-time plots were collected in solutions identical to the CV solution conditions with the addition of stirring at a rate of 1000 rpm.

In aqueous media, the $Ru^V{=}O^{3+}$ oxidation state of nanoITO|**1-PO$_3$H$_2$**, nanoITO|$Ru^V{=}O^{3+}$, undergoes nucleophilic attack by a water molecule with concerted proton transfer to a second water molecule by atom–proton transfer (APT) (eq 1). This APT step results in a hydroperoxide intermediate,

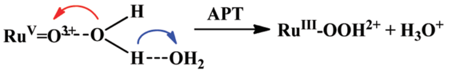

(1)

$Ru^{III}{-}OOH^{2+}$.[14,15] This intermediate undergoes oxidation to $Ru^{IV}(OO)^{2+}$ with slow O_2 release or further oxidation to the reactive peroxide, $Ru(OO)^{3+}$, which rapidly evolves O_2.[11] On the basis of DFT analysis, both of the peroxide intermediates have six-coordinate "open" and seven-coordinate "closed" forms, with the latter favored for $Ru^{IV}(OO)^{2+}$ and the former for $Ru^V(OO)^{3+}$.[13,14]

There is evidence for Ru peroxide formation on the surface of nanoITO|**1-PO$_3$H$_2$**, in aqueous solutions, following an oxidative scan past the $Ru^{IV}{=}O^{2+} \rightarrow Ru^V{=}O^{3+}$ wave in the appearance of new pH-dependent waves attributable to the peroxide couples, $Ru^{III}{-}OOH^{2+}/Ru^{II}(HOOH)^{2+}$ and $Ru^{IV}(OO)^{2+}/Ru^{III}{-}OOH^{2+}$;[11,13] however, in PC with 1% water by volume, there is no evidence for peroxide formation on the surface, possibly because of minimal water oxidation occurring in PC at low water concentrations. In a previous study, it was shown that the rate of water oxidation in PC/water mixtures varies linearly with the concentration of added water.[12]

2. SURFACE ELECTROCHEMISTRY

The dashed line CV in Figure 1 and Figure S1 in the Supporting Information show a voltammogram of nanoITO|**1-PO$_3$H$_2$** in PC/1% water. As shown in an earlier study, CV responses for the surface PCET couples, $Ru^{III}{-}OH^{2+}/Ru^{II}{-}OH_2^{2+}$ and $Ru^{IV}{=}O^{2+}/Ru^{III}{-}OH^{2+}$, in PC/water include contributions from the surface-bound phosphonate groups that have pK_a values of ~1–2.[22] In contrast to aqueous solutions in which proton equilibration between the phosphonate groups and the surrounding solution occurs rapidly, in PC, the surface proton composition is "fixed" due to slow proton equilibration.[15] In this environment, the initial oxidative wave at $E_{1/2}$ = 0.76 V is due to incomplete oxidation of $Ru^{II}{-}OH_2^{2+}$ to $Ru^{III}{-}OH^{2+}$ at the thermodynamic potential for the couple. The partial nature of the oxidation arises from a kinetic inhibition to proton transfer to or from the phosphonate groups apparently arising from distance and orientation effects.[15] The remaining Ru(II) sites are oxidized at $E_{1/2}$ = 1.03 V for the $Ru^{III}{-}OH_2^{3+}/Ru^{II}{-}OH_2^{2+}$ couple. In the dashed line CV of Figure 1, the shoulder at $E_{p,a}$ ~ 1.3 V on the anodic wave at $E_{p,a}$ = 1.62 V is attributed to the $Ru^{IV}{=}O^{2+}/Ru^{III}{-}OH^{2+}$ couple, which is also kinetically inhibited.[15] The wave at 1.62 V coincides with the $E_{p,a}$ for the $Ru^V{=}O^{3+}/Ru^{IV}{=}O^{2+}$ couple with the enhanced current due to oxidation of the remaining sites on the surface from lower oxidation states, Ru(IV) and Ru(III), to $Ru^V{=}O^{3+}$, plus a small contribution from water oxidation.

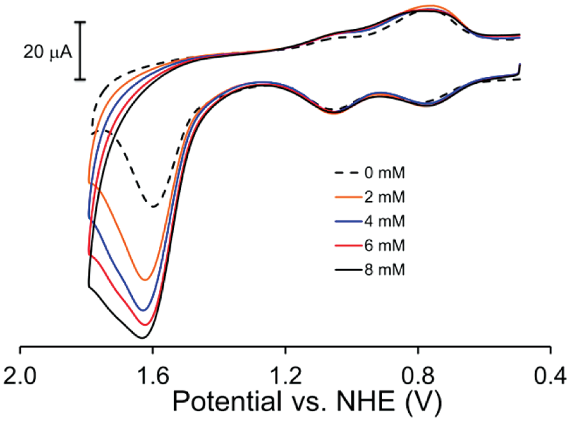

Figure 1. Overlaid CVs of nanoITO|**1-PO$_3$H$_2$** at 10 mV/s (I = 0.1 M $LiClO_4$ T = 23 ± 2 °C) in the presence of increasing amounts of ethylbenzene displaying the electrocatalytic activity of the catalyst toward ethylbenzene oxidation.

3. ELECTROCATALYTIC OXIDATION OF HYDROCARBONS

Addition of aliquots of ethylbenzene to PC/1% water resulted in incremental increases in $i_{p,a}$ at ≈1.6 V (Figure 1). This response is consistent with electrocatalytic oxidation of ethylbenzene by nanoITO|$Ru^V{=}O^{3+}$. There is no change in the current response for the $Ru^{III}{-}OH_2^{3+}/Ru^{II}{-}OH_2^{2+}$ and $Ru^{III}{-}OH^{2+}/Ru^{II}{-}OH_2^{2+}$ couples, indicating lower oxidation states of the catalyst are not active toward ethylbenzene oxidation on the CV time scale.

To determine the product of electrocatalytic oxidation, controlled potential electrolysis of nanoITO|**1-PO$_3$H$_2$** was performed in PC/1% H_2O (I = 0.1 M $LiClO_4$, area = 1 cm^2, T = 23 ± 2 °C) in the presence of 20 mM ethylbenzene at 1.74 V. A current density of ≈4000 mA/cm^3 was maintained for 12 h. Liquid injection GC analysis compared with standards showed that 1.6×10^{-5} mol of acetophenone was produced during the electrolysis, corresponding to a 95% faradic efficiency. GC/MS analysis further confirmed the 4 e^- oxidized product. Very minor peaks (<1% of the integrated area for acetophenone) were observed in the liquid injection GC analysis, but the identity of these peaks has yet to be determined.

Catalytic rate constants were evaluated by steady state current measurements[20] at 1.74 V vs NHE by application of eqs 2 and 3 to the data in Figure 2. In the equations, i_{cat} is the steady state current, n_{cat} (= 4) is the electronic stoichiometry for ethylbenzene oxidation to acetophenone, and F is the Faraday constant.

$$i_{cat} = n_{cat} F V \Gamma k_{cat} \tag{2}$$

$$k_{cat} = k_{oxEB}[\text{ethylbenzene}] \tag{3}$$

Γ is the surface coverage for the fully loaded electrode (1.0×10^{-8} mol/cm^2, 2.5 μm thickness), V is the volume of the electrode, and k_{cat} is the catalytic rate constant. From the plot of i_{cat} vs [ethylbenzene] in the inset in Figure 2, k_{cat} is first-order in ethylbenzene consistent with the rate law in eq 3 with k_{oxEB} = 2.5 ± 0.2 M^{-1} s^{-1} (I = 0.1 M $LiClO_4$, 23 ± 2 °C). When compared, experiments performed under a N_2 atmosphere and

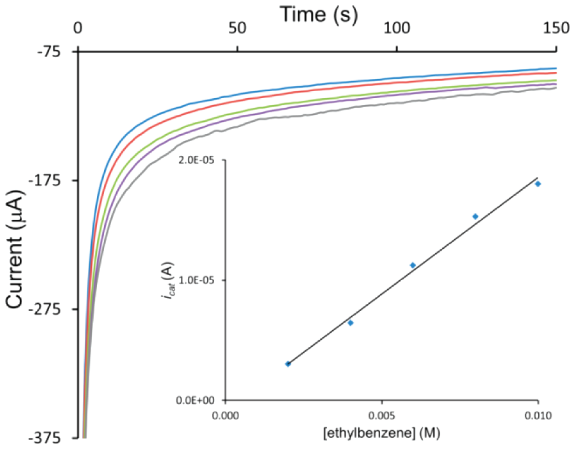

Figure 2. Current versus time curves for nanoITO|**1-PO$_3$H$_2$** in the presence of 2, 4, 6, 8, and 10 mM ethylbenzene at 1.74 V (PC/1% H_2O, I = 0.1 M $LiClO_4$, 23 ± 2 °C). Inset: linear dependence of background-subtracted steady-state current (i_{cat}) at 150 s versus ethylbenzene concentration.

experiments performed open to an air atmosphere showed no significant differences in i_{cat}, suggesting that the presence of O_2 does not significantly affect the catalytic mechanism.

A H/D kinetic isotope effect (KIE) value was determined by repeating the electrochemical kinetics experiments with ethylbenzene-d_{10}. On the basis of the results of these experiments, k_{C8D10} = 2.0 ± 0.4 M^{-1} s^{-1} with k_{C8H10}/k_{C8D10} = 1.2 ± 0.2 in PC/1% H_2O (I = 0.1 M $LiClO_4$, 23 ± 2 °C). The small magnitude of the KIE value is inconsistent with a mechanism involving hydride or hydrogen atom transfer (HAT) from ethylbenzene to the oxidant in the rate-limiting step. Direct O-atom insertion mechanisms with relatively small H/D KIE magnitudes have been reported,[23] and alkyl aromatic oxidations by related Ru(O) catalysts that undergo HAT mechanisms exhibit H/D KIE as great as 49.[6] The absence of an O_2 effect is also incompatible with a hydrogen atom transfer mechanism because HAT mechanisms generate radical intermediates that are sensitive to dissolved O_2 in solution.[7]

A mechanism consistent with the experimental observations is shown in eqs 4a–d (Scheme 2). The mechanism features rate-limiting O-atom insertion into a C–H bond to give an intermediate with 1-phenylethanol in the coordination sphere (eq 4a). Once formed, this 2e$^-$ intermediate undergoes further 2e$^-$/2H$^+$ oxidation to the coordinated ketone, followed by solvolysis. A related oxygen atom insertion mechanism for benzyl alcohol oxidation to benzaldehyde has been shown with UV–vis observation of an O-atom insertion intermediate.[17]

There is no evidence in the controlled potential electrolysis experiments for buildup of the intermediate alcohol, 1-phenylethanol. This, and the results of rate measurements (Supporting Information), which show that nanoITO|Ru^V=O^{3+} oxidation of the alcohol occurs with k ~ 7.5 M^{-1} s^{-1}, are consistent with oxidation of the alcohol in the coordination sphere of the intermediate in eq 4b before it undergoes solvolysis (eq 4c).

Scheme 2. Proposed Oxygen Atom Insertion Mechanism for Electrocatalytic Ethylbenzene Oxidation by nanoITO|Ru^V=O^{3+}

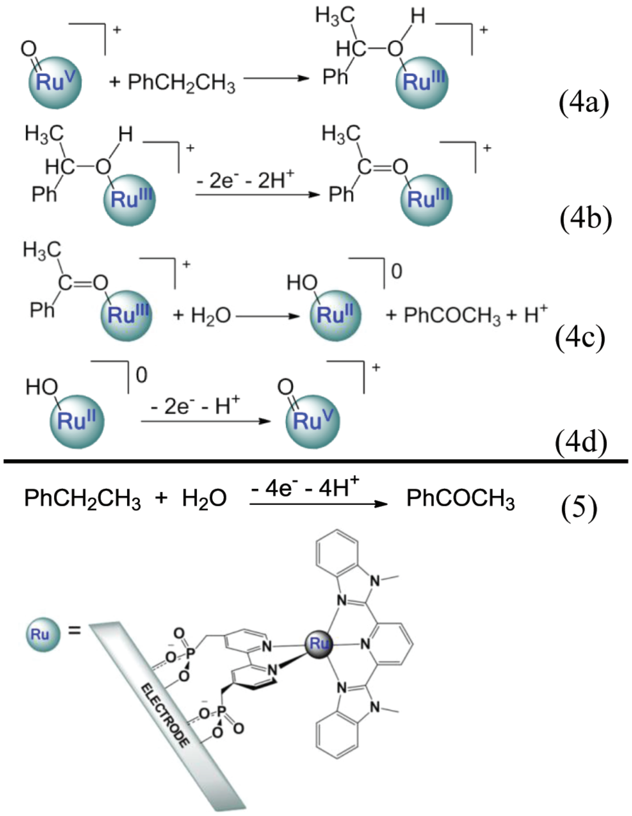

Initial studies on the electrocatalytic oxidation of toluene and cumene by nanoITO|**1-PO$_3$H$_2$** exhibit similar reactivity compared with ethylbenzene, with steady state current measurements shown in the Supporting Information. Product yield and kinetic isotope effect studies are currently under investigation for both reactions. The catalyst did not exhibit any catalytic activity in the presence of cyclohexane at room temperature. This was an expected result, because the BDE of a C–H bond in cyclohexane is 99.5 kcal/mol,[24] and the estimated BDE of Ru^V=O + H· is roughly 95 kcal/mol.[25]

4. CONCLUSIONS

Our results are important in describing a general, high-surface-area, heterogeneous electrocatalytic method for efficient hydrocarbon oxidation/activation. Oxidation occurs by mechanistically well-defined steps with product control and high faradic efficiencies at diffusionally restricted oxidation sites on an oxide electrode surface. Oxidative activation by PCET gives a reactive intermediate in a mixed solvent environment, which limits competitive water oxidation but provides water for sustaining the catalytic cycle. The key and advantageous mechanistic step appears to be net O-atom insertion into a C–H bond, allowing for selectivity by avoiding H atom transfer from C–H bonds and high-energy radical intermediates, which have been shown to lead to a mixture of products with low faradic efficiencies. In current experiments, we are investigating the reactivity of surface-bound catalysts toward saturated hydrocarbons.

■ ASSOCIATED CONTENT

Ⓢ Supporting Information

Additional information as noted in the text. This material is available free of charge via the Internet at http://pubs.acs.org.

AUTHOR INFORMATION

Corresponding Author

*Phone: 919-843-8313. Fax: 919-962-2388. E-mail: tjmeyer@unc.edu.

Notes

The authors declare no competing financial interest.

ACKNOWLEDGMENTS

Dedicated to Hubert Le Bozec and all of his accomplishments for his 60th birthday. Funding by the Center for Catalytic Hydrocarbon Functionalization an Energy Frontier Research Center (EFRC) funded by the U.S. Department of Energy, Office of Science, Office of Basic Energy Sciences, under Award DE-SC0001298 supporting the electrochemical experiments of A.K.V. and the UNC EFRC Solar Fuels, an EFRC funded by the U.S. Department of Energy, Office of Science, Office of Basic Energy Sciences, under Award DE-SC0001011 for supporting J.J.C. for the synthesis of the compound and Z.C. for development of techniques is gratefully acknowledged. We also acknowledge support from the Army Research Office through Grant W911NF-09-1-0426 (to A.K.V.) for product analysis. Acknowledgment also goes for the purchase of the instrumentation from UNC EFRC (Solar Fuels, an Energy Frontier Research Center funded by the U.S. Department of Energy, Office of Science, Office of Basic Energy Sciences under Award Number DE-SC0001011) and from UNC SERC (Solar Energy Research Center Instrumentation Facility, funded by the U.S. Department of Energy, Office of Energy Efficiency & Renewable Energy, under Award Number DE-EE0003188).

REFERENCES

(1) Che, C.; Zhang, J.; Zhang, R.; Huang, J.; Lai, T.; Tsui, W.; Zhou, X.; Zhou, Z.; Zhu, N.; Chang, C. K. *Chem.—Eur. J.* **2005**, *11*, 7040–7053.

(2) Brown, E. S.; Robinson, J. R.; McCoy, A. M.; McGaff, R. W. *Dalton Trans.* **2011**, *40*, 5921–5925.

(3) Fernández, T. L.; Souza, E. T.; Visentin, L. C.; Santos, J. V.; Mangrich, A. S.; Faria, R. B.; Antunes, O. A. C.; Scarpellini, M. *J. Inorg. Biochem.* **2009**, *103*, 474–479.

(4) Larsen, A. S.; Wang, K.; Lockwood, M. A.; Rice, G. L.; Won, T.; Lovell, S.; Sadilek, M.; Turecek, F.; Mayer, J. M. *J. Am. Chem. Soc.* **2002**, *124*, 10112–10123.

(5) Lee, S.; Han, J.; Kwak, H.; Lee, S.; Lee, E.; Kim, H.; Lee, J.; Bae, C.; Lee, S.; Kim, Y.; Kim, C. *Chem.—Eur. J.* **2007**, *13*, 9393–9398.

(6) Kojima, T.; Nakayama, K.; Ikemura, K.; Ogura, T.; Fukuzumi, S. *J. Am. Chem. Soc.* **2011**, *133*, 11692–11700.

(7) Bryant, J. R.; Matsuo, T.; Mayer, J. M. *Inorg. Chem.* **2004**, *43*, 1587–1592.

(8) Ozawa, H.; Hino, T.; Ohtsu, H.; Wada, T.; Tanaka, K. *Inorg. Chim. Acta* **2011**, *366*, 298–302.

(9) Hughes, M. D.; Xu, Y.; Jenkins, P.; McMorn, P.; Landon, P.; Enache, D. I.; Carley, A. F.; Attard, G. A.; Hutchings, G. J.; King, F.; Stitt, E. H.; Johnston, P.; Griffin, K.; Kiely, C. J. *Nature* **2005**, *437*, 1132–1135.

(10) Chen, Z.; Concepcion, J. J.; Hull, J. F.; Hoertz, P. G.; Meyer, T. J. *Dalton Trans.* **2010**, *39*, 6950.

(11) Chen, Z.; Concepcion, J. J.; Jurss, J. W.; Meyer, T. J. *J. Am. Chem. Soc.* **2009**, *131*, 15580–15581.

(12) Chen, Z.; Concepcion, J. J.; Luo, H.; Hull, J. F.; Paul, A.; Meyer, T. J. *J. Am. Chem. Soc.* **2010**, *132*, 17670–17673.

(13) Concepcion, J. J.; Tsai, M.; Muckerman, J. T.; Meyer, T. J. *J. Am. Chem. Soc.* **2010**, *132*, 1545–1557.

(14) Concepcion, J. J.; Jurss, J. W.; Templeton, J. L.; Meyer, T. J. *J. Am. Chem. Soc.* **2008**, *130*, 16462–16463.

(15) Chen, Z.; Vannucci, A. K.; Concepcion, J. J.; Jurss, J. W.; Meyer, T. J. *Proc. Natl. Acad. Sci.* **2011**, *108*, E1461–E1469.

(16) Paul, A.; Hull, J. F.; Norris, M. R.; Chen, Z.; Ess, D. H.; Concepcion, J. J.; Meyer, T. J. *Inorg. Chem.* **2011**, *50*, 1167–1169.

(17) Vannucci, A. K.; Hull, J. F.; Chen, Z.; Binstead, R. A.; Concepcion, J. J.; Meyer, T. J. *J. Am. Chem. Soc.* **2012**, *134*, 3972–3975.

(18) Thompson, M. S.; Meyer, T. J. *J. Am. Chem. Soc.* **1982**, *104*, 5070–5076.

(19) Concepcion, J. J.; Jurss, J. W.; Norris, M. R.; Chen, Z.; Templeton, J. L.; Meyer, T. J. *Inorg. Chem.* **2010**, *49*, 1277.

(20) Hoertz, P. G.; Chen, Z.; Kent, C. A.; Meyer, T. J. *Inorg. Chem.* **2010**, *49*, 8179–8181.

(21) Peppel, W. J. *Ind. Eng. Chem.* **1958**, *50*, 767–770.

(22) Gagliardi, C. J.; Jurss, J. W.; Thorp, H. H.; Meyer, T. J. *Inorg. Chem.* **2011**, *50*, 2076–2078.

(23) Murray, R. W.; Jeyaraman, R.; Mohan, L. *J. Am. Chem. Soc.* **1986**, *108*, 2470–2472.

(24) Luo, Y.-R. *Handbook of Bond Dissociation Energies in Organic Compounds*; CRC Press: Boca Raton, FL, 2003.

(25) Parker, V. D. *J. Am. Chem. Soc.* **1992**, *114*, 7458.